

Analyt. Näherung für  $t_{\text{cor}}(D)$  für Van der Pol-Oszillator  
 (mean-field Näherung, Pomplun et al., Europhys. Lett. 71, 366 (2005))

Näherung für  $D \ll |E|/\omega_0$ :  $\langle x^2 \rangle$  klein

$$\varepsilon - x^2 \approx \varepsilon - \langle x^2 \rangle = \tilde{\varepsilon} < 0$$

$$\rightarrow \begin{cases} \dot{x} = y \\ \dot{y} = \tilde{\varepsilon} y - \omega_0^2 x + D \xi(t) \end{cases}$$

lin. stoch. Dgl. (multivariate Ornstein-Uhlenbeck-Prozess)  
 stationäre  $\langle x_s \rangle = 0$

$$d\underline{x}_s = -\underline{A} \underline{x}_s dt + \underline{B} d\underline{W}(t) \quad \underline{x}_s = \begin{pmatrix} x \\ y \end{pmatrix} \quad \underline{A} = \begin{pmatrix} 0 & -1 \\ \omega_0^2 & -\tilde{\varepsilon} \end{pmatrix}$$

$$\underline{B} = \begin{pmatrix} 0 & 0 \\ 0 & D \end{pmatrix}$$

Varianz-Matrix

$$\underline{\Sigma} = \langle \underline{x}_s(t) \otimes \underline{x}_s(t) \rangle = \frac{D^2}{-2\tilde{\varepsilon}} \begin{pmatrix} \frac{1}{\omega_0^2} & 0 \\ 0 & 1 \end{pmatrix}$$

$$\Rightarrow \langle x^2 \rangle = \frac{D^2}{-2\tilde{\varepsilon} \omega_0^2} = \frac{D^2}{-2(\varepsilon - \langle x^2 \rangle) \omega_0^2}$$

selbstkonsistente Lösung von  $\langle x^2 \rangle$  in Abh. von  $D$

$$\langle x^2 \rangle^2 - \varepsilon \langle x^2 \rangle - \frac{D^2}{2\omega_0^2} = 0$$

$$\langle x^2 \rangle = \frac{\varepsilon}{2} (+) \frac{\varepsilon}{2} \sqrt{1 + \frac{2D^2}{\varepsilon^2 \omega_0^2}} \quad (+) \text{ unphys. Lsg., da } \langle x^2 \rangle \geq 0$$

$$\Rightarrow \tilde{\varepsilon} = \varepsilon - \langle x^2 \rangle = \frac{\varepsilon}{2} \left( 1 + \sqrt{1 + \frac{2D^2}{\varepsilon^2 \omega_0^2}} \right)$$

Dämpfung  $\tilde{\varepsilon}$  = Abstand zur Hopf-Bif.  
 wächst mit Rauschintensität  $D$ !

Autokorr.fkt. für linearen stoch. Prozess

$$\Phi_{yy}(s) = \langle y(t+s)y(t) \rangle \approx \Phi_{yy}(0) e^{ps} \cos \tilde{\omega}s$$

wobei  $\lambda_{1,2} = p \pm i\tilde{\omega} = \frac{p}{2} \pm i\sqrt{\omega_0^2 - \frac{p^2}{4}}$  die Eigenwerte von A sind.

$$\Rightarrow t_{cor} = \frac{1}{\Phi(0)} \int_0^\infty |\Phi(s)| ds \approx \frac{2}{\pi} \int_0^\infty e^{ps} ds = -\frac{2}{\pi p}$$



Frequenz

$$\Rightarrow t_{cor}(D) \approx \frac{4}{\pi |\tilde{\omega}(D)|}$$

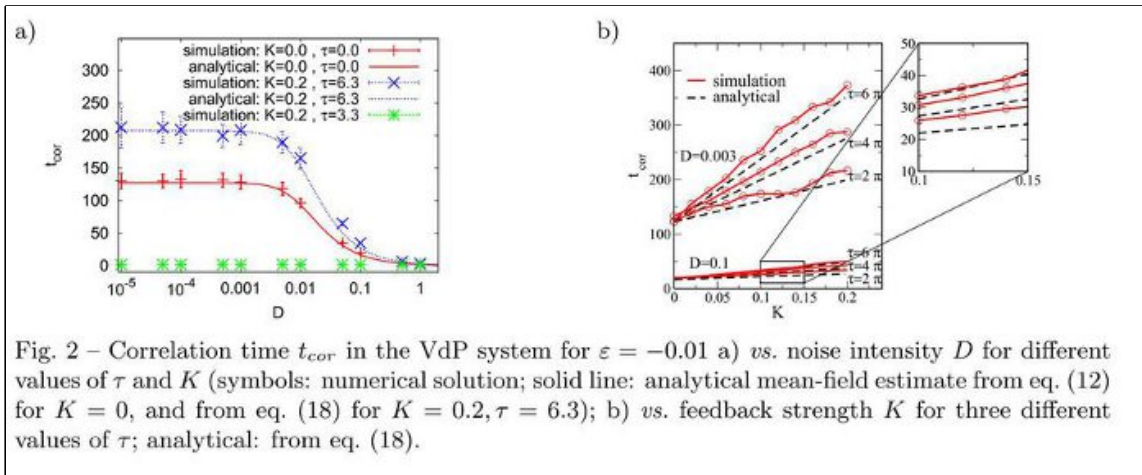


Fig. 2 - Correlation time  $t_{cor}$  in the VdP system for  $\varepsilon = -0.01$  a) vs. noise intensity  $D$  for different values of  $\tau$  and  $K$  (symbols: numerical solution; solid line: analytical mean-field estimate from eq. (12) for  $K = 0$ , and from eq. (18) for  $K = 0.2, \tau = 6.3$ ); b) vs. feedback strength  $K$  for three different values of  $\tau$ ; analytical: from eq. (18).

Pomplun et al (2005)

## Spektrale Leistungsdiichte

Fourier-Transf. der mean-field-Gl.:  $\dot{x} = f$   
 $\dot{y} = \tilde{\omega}y - \omega_0^2 x + D\xi(t)$   
 $(x(t) = \int_{-\infty}^{\infty} d\omega e^{-i\omega t} \hat{x}(\omega))$

$$-i\omega \hat{x}(\omega) = \hat{y}(\omega)$$

$$-i\omega \hat{y}(\omega) = \tilde{\omega} \hat{y}(\omega) - \omega_0^2 \hat{x}(\omega) + D \hat{\xi}(\omega)$$

Elim. von  $\hat{x}(\omega) = \frac{i}{\omega} \hat{y}(\omega)$ :

$$-i\omega \hat{y} - \tilde{\omega} \hat{y} + i \frac{\omega_0^2}{\omega} \hat{y} = D \hat{\xi} \quad | : i\omega$$

$$\hat{y}(\omega) = \frac{i\omega D \xi(\omega)}{\omega^2 - \omega_0^2 - i\omega \tilde{\epsilon}}$$

$$\langle \hat{y}(\omega) \hat{y}^*(\omega') \rangle = \frac{(i\omega D) (-i\omega' D) \langle \xi(\omega) \xi^*(\omega') \rangle}{(\omega^2 - \omega_0^2 - i\omega \tilde{\epsilon}) (\omega'^2 - \omega_0^2 + i\omega' \tilde{\epsilon})}$$

$$\begin{aligned} \langle \xi(\omega) \xi^*(\omega') \rangle &= \frac{1}{(2\pi)^2} \int_{-\infty}^{\infty} dt e^{i\omega t} \int_{-\infty}^{\infty} dt' e^{-i\omega' t'} \underbrace{\langle \xi(t) \xi(t') \rangle}_{\delta(t-t')} \\ &= \frac{1}{2\pi} \cdot \frac{1}{2\pi} \int_{-\infty}^{\infty} dt e^{i(\omega - \omega')t} \\ &\quad \underbrace{\hspace{10em}}_{\delta(\omega - \omega')} \end{aligned}$$

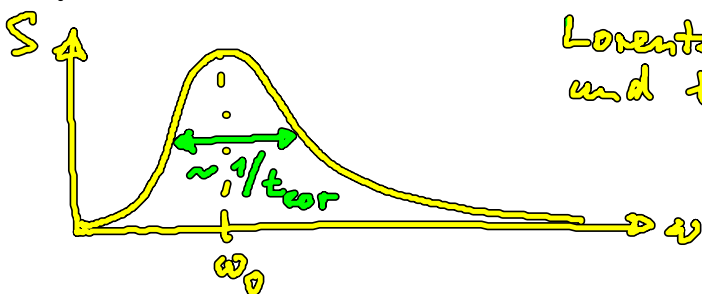
R.S.:  $\omega = \omega'$

$$\Rightarrow \langle \hat{y}(\omega) \hat{y}^*(\omega') \rangle = \frac{D^2}{2\pi} \frac{\omega^2 \delta(\omega - \omega')}{(\omega^2 - \omega_0^2)^2 + \omega^2 \tilde{\epsilon}^2}$$

andererseits mit Wiener-Khinchin-Theorem:

$$\begin{aligned} \langle \hat{y}(\omega) \hat{y}^*(\omega') \rangle &= \frac{1}{(2\pi)^2} \int_{-\infty}^{\infty} dt e^{i\omega t} \int_{-\infty}^{\infty} dt' e^{-i\omega' t'} \langle y(t) y(t') \rangle \\ &= \frac{1}{2\pi} \int_{-\infty}^{\infty} dt e^{i(\omega - \omega')t} \underbrace{\frac{1}{2\pi} \int_{-\infty}^{\infty} ds e^{i\omega' s} \langle y(t) y(t+s) \rangle}_{\delta(\omega')} \end{aligned}$$

$$S_{yy}(\omega) = \frac{D^2}{2\pi} \frac{\omega^2}{(\omega^2 - \omega_0^2)^2 + \omega^2 \tilde{\epsilon}^2}$$



Lorentzkurve mit Max. bei  $\omega_0$   
und Halbwertsbreite  $\approx \frac{|\tilde{\epsilon}|}{2} = \frac{2}{\pi \tau_{0r}(D)}$

# Analys. Näherung für Fitzhugh-Nagumo-Modell:

Prager, Lehel, Schimansky-Gier, Schöll, J. Phys. A 40, 11045 (2007)  
Konvari, Schimansky-Gier, Schöll: Eur. Phys. J. ST (2010/11)  
2-state Master-gl.

## gekoppelte Fitzhugh-Nagumo-Systeme mit Rauschen

Hauschildt, Balcerow, Janson, Schöll: PRL 77, 051906 (2006)  
Hövel, Dallen, Schöll: Int. J. Exp. Chaos 20, 813 (2010)

## stochastische Synchronisation

farbiges Rauschen:  $\langle \eta(t) \eta(t') \rangle = \sigma^2 e^{-|t-t'|/\tau_c}$

⇔ generiert durch Ornstein-Uhlenbeck-Prozess

$$\tau_c \dot{\eta} = -\eta + \sqrt{2\sigma^2 \tau_c} \xi(t) \quad \langle \xi(t) \xi(t') \rangle = \delta(t-t')$$

Brandstetter, Dallen, Schöll: Phil. Trans. R. Soc. A 368, 331 (2010)

## 3. Beispiel: SNIPER-Modell (Anregbarkeit Typ I)

- knapp unterhalb einer globalen Bif. (Ampl. endl.,  $\omega \rightarrow 0$ )  
Hopf: Ampl.  $\rightarrow 0$ ,  $\omega$  endl.

SNIPER  $\hat{=}$  saddle-node infinite period bif.

$\hat{=}$  SNIC  $\hat{=}$  saddle-node bif. on invariant cycle

$\hat{=}$  Sattel-Knoten-Bif. auf Grenzzyklen

Gang et al.: PRL 71, 807 (1993): Kohärenzresonanz erstmal  
Aust, Hövel, Kizamide, Schöll: Eur. Phys. J. ST 187, 77 (2010)  
mit delay

$$\begin{aligned} \dot{x} &= x(1-x^2-y^2) + y(x-b) + D\xi(t) \\ \dot{y} &= y(1-x^2-y^2) - x(x-b) + D\xi(t) \end{aligned}$$

$D=0$

$$\begin{aligned} \dot{r} &= r(1-r^2) \\ \dot{\varphi} &= b - r \cos \varphi \end{aligned}$$

$$\begin{aligned} x &= r \cos \varphi \\ y &= r \sin \varphi \end{aligned}$$

Fixp. (i)  $r=0$  (instab. Fokus)

(ii)  $r=1$ ,  $\varphi = \arccos b$  (Sattelp. S)  
(iii)  $r=1$ ,  $\varphi = -\arccos b$  (stab. Knoten N) } ex. falls  $b < 1$

$b = 1$  : Sattel-Knoten-Bif. auf dem invarianten Kreis  $r=1$   
 ( $r=1, \dot{r}=0, \dot{\varphi} = b - \cos\varphi$ ) bei  $\varphi=0$

$b > 1$  : Grenzzyklus  $r=1, \int \frac{d\varphi}{b - \cos\varphi} = t \Rightarrow \varphi(t)$  analyt.  
 $T = \frac{2\pi}{\sqrt{b^2 - 1}} \xrightarrow{b \rightarrow 1} \infty$

Anregbares Regime :  $b < 1$

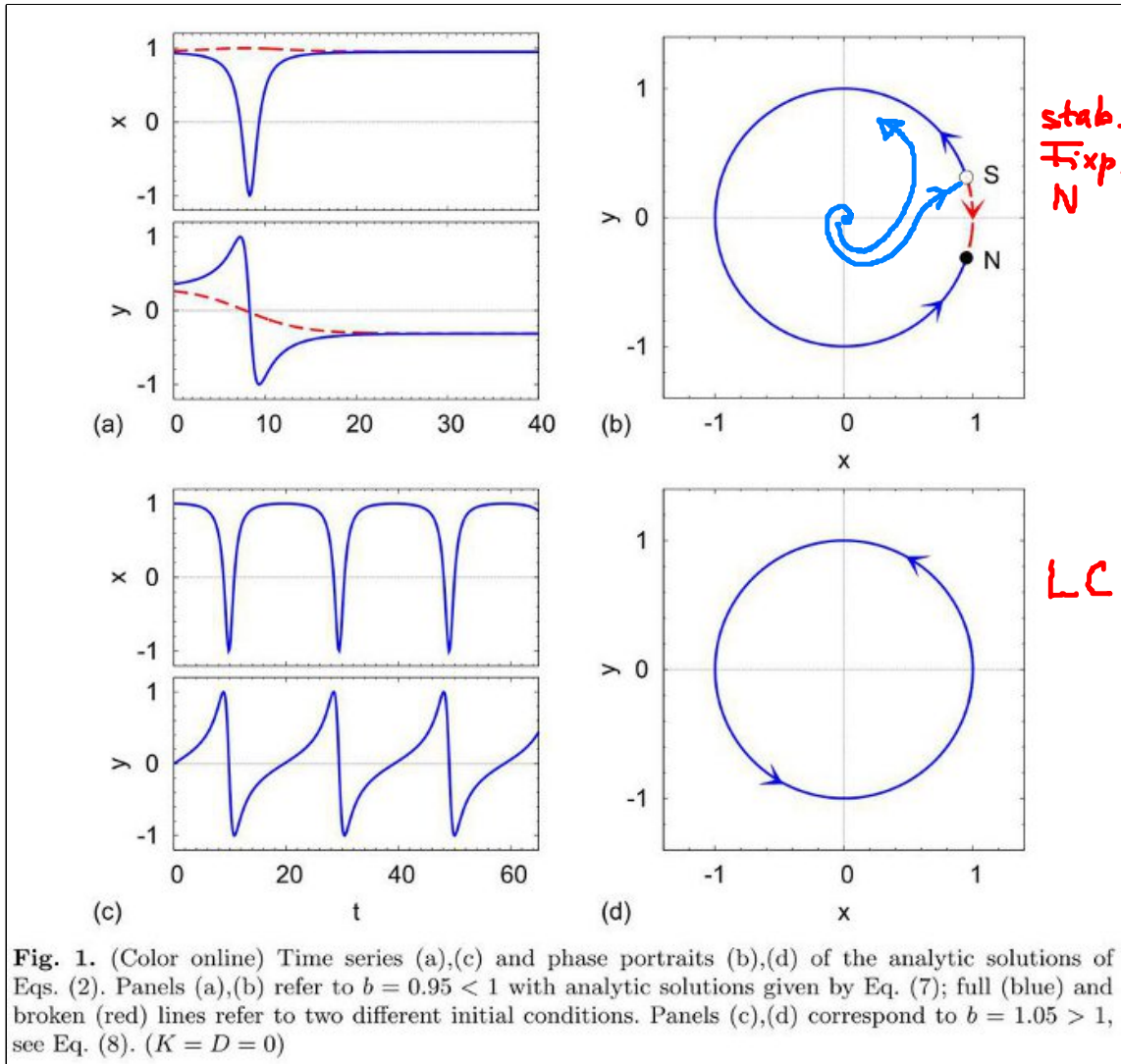


Fig. 1. (Color online) Time series (a),(c) and phase portraits (b),(d) of the analytic solutions of Eqs. (2). Panels (a),(b) refer to  $b = 0.95 < 1$  with analytic solutions given by Eq. (7); full (blue) and broken (red) lines refer to two different initial conditions. Panels (c),(d) correspond to  $b = 1.05 > 1$ , see Eq. (8). ( $K = D = 0$ )

$D \neq 0$  : Kohärenzmodulation

Anst et al  
(2010)

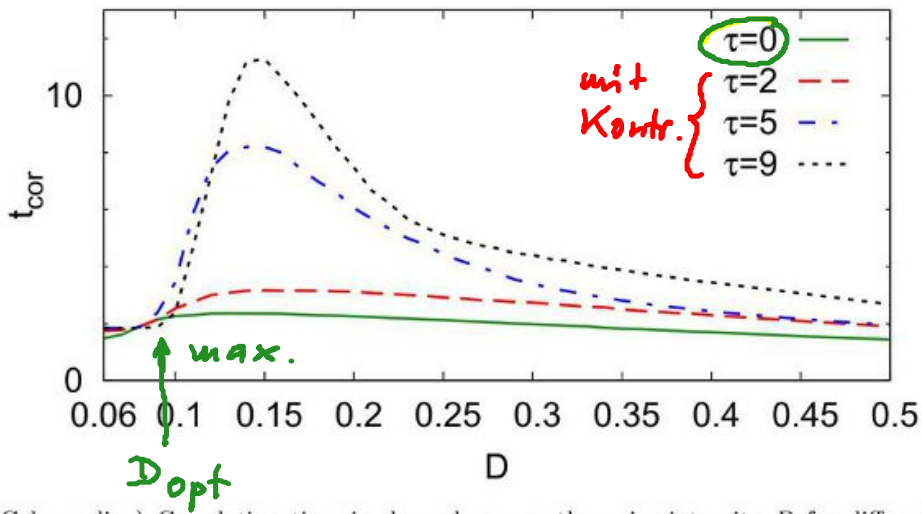


Fig. 4. (Color online) Correlation time in dependence on the noise intensity  $D$  for different time delays  $\tau$ . The solid (green) curve corresponds to the uncontrolled system ( $\tau = 0$ ). The dashed (red), dash-dotted (blue), and dotted (black) curves refer to values of  $\tau = 2, 5$ , and  $9$ , respectively. Other parameters:  $b = 0.95$  and  $K = 0.25$ .

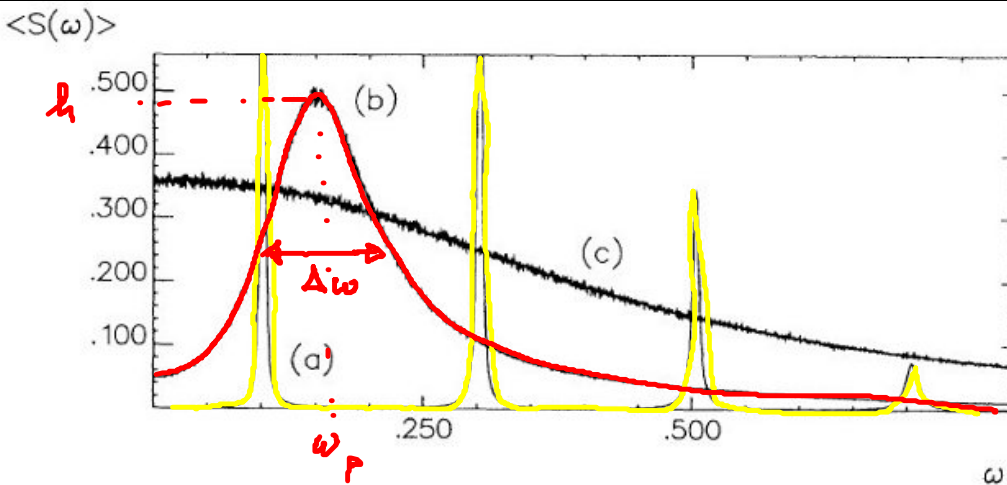


FIG. 1. The averaged power spectrum of  $y(t)$  for  $b = 1.05$  and various  $D$ . A limit cycle exists for the deterministic system. (a)  $D = 0.00003$ . (b)  $D = 0.05$ . (c)  $D = 0.9$ .

Gang et al  
PRL (1993)

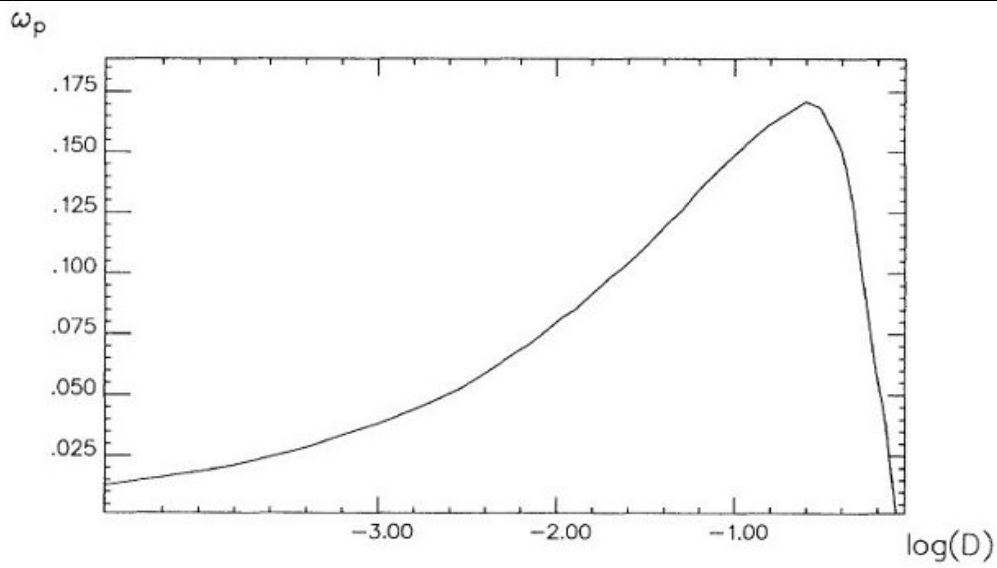


FIG. 3. The center frequency of the spectrum peak  $\omega_p$  vs  $\log(D)$  with  $b=1$  (the same in Figs. 4 and 5).

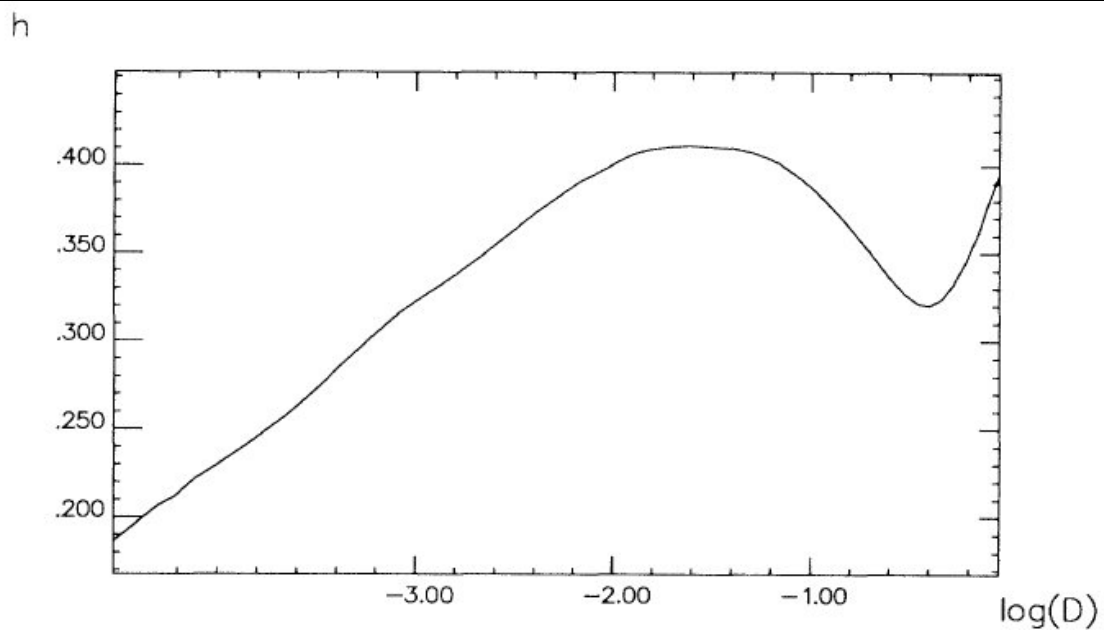


FIG. 4. The spectrum peak height  $h$  plotted against  $\log(D)$ . A resonancelike curve is obvious. However,  $h$  goes up again for very large  $D$ .

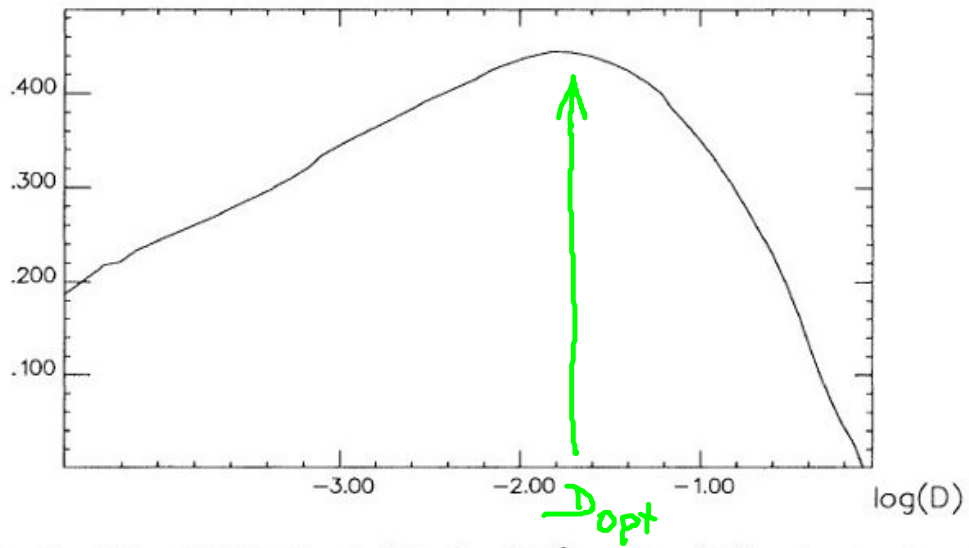
$\beta$ 

FIG. 5. The SNR  $\beta = h(\Delta\omega/\omega_p)^{-1}$  vs  $\log(D)$ . A stochastic resonance maximum can be seen.